

## HeteroTOCSY-based experiments for measuring heteronuclear relaxation in nucleic acids and proteins

Barry I. Schweitzer<sup>a,\*</sup>, Kevin H. Gardner<sup>c</sup> and Gregory Tucker-Kellogg<sup>b,c,\*\*</sup>

<sup>a</sup>*Department of Pediatrics, Yale University School of Medicine, <sup>b</sup>Department of Chemistry and <sup>c</sup>Department of Molecular Biophysics and Biochemistry, Yale University, New Haven, CT 06510-8064, U.S.A.*

Received 21 December 1994

Accepted 12 May 1995

*Keywords:* DNA; Phosphorus; Cadmium; Heteronuclear; Relaxation; HeteroTOCSY; Cytosine arabinoside; LAC9

### Summary

While both <sup>31</sup>P and <sup>113</sup>Cd are present at locations of interest in many different macromolecular systems, heteronuclear-detected relaxation measurements on these nuclei have been restrained by limitations in either resolution or signal-to-noise ratio. We have developed heteroTOCSY-based methods to overcome both of these problems. Two-dimensional versions of these experiments were utilized to measure <sup>31</sup>P T<sub>1</sub> and T<sub>2</sub> values in DNA oligonucleotides; the additional resolution offered by a second dimension allowed determination of these values for most of the <sup>31</sup>P resonances in a DNA dodecamer. The results from the experiments indicated that there was little significant variation in T<sub>1</sub> values for the different phosphates in the DNA dodecamer; however, the T<sub>2</sub> values showed a clear pattern, with lower values in the interior of the sequence than at the ends of the helix. Furthermore, a significant correlation between <sup>31</sup>P chemical shifts and T<sub>2</sub> values was observed. One-dimensional, frequency-selective versions of these experiments were also developed for use on systems containing a smaller number of heteronuclear spins. These methods were applied to investigate the heteronuclear relaxation properties of <sup>113</sup>Cd in <sup>113</sup>Cd<sub>2</sub>LAC9(61), a Cys<sub>6</sub>Zn<sub>2</sub> DNA-binding domain. Data from the experiments confirm biochemical evidence that more significant differences occur in the metal-protein interactions between the two metal-binding sites than has been previously identified for proteins containing this motif.

### Introduction

Solution NMR studies of <sup>15</sup>N and <sup>13</sup>C relaxation rates have been applied to many protein systems to examine backbone and side-chain dynamics. A key to the success of this approach has been the development of a large number of proton-detected multidimensional experiments to obtain the relevant information. This class of experiment offers two main advantages over directly detected versions: (1) enhanced sensitivity, due to the large gyromagnetic ratio of <sup>1</sup>H, and (2) improved resolution, resulting from the ability to separate peaks with two different chemical shifts.

Although these methods are commonly used in studies of <sup>15</sup>N and <sup>13</sup>C nuclei, investigations of the relaxation properties of other biologically relevant spin-1/2 nuclei,

including phosphorus-31 and cadmium-113, could benefit from a similar approach. <sup>31</sup>P is present in the phosphodiester backbones of RNA and DNA, a key location for probing dynamics along the length of these molecules. <sup>113</sup>Cd has been substituted into binding sites in proteins for a wide variety of metals, including zinc, calcium and iron. Hence, both nuclei are present at locations of particular interest in many different macromolecular systems. The two nuclei also have similar NMR characteristics, including relatively high gyromagnetic ratios and chemical shift anisotropy (CSA) dominance of their relaxation mechanisms in many biological environments. Additionally, prior heteronuclear-detected relaxation studies of these nuclei in model compounds and macromolecules provide a database of information for comparative studies.

Previous <sup>31</sup>P and <sup>113</sup>Cd relaxation measurements have

\*To whom correspondence should be addressed at: Walt Disney Memorial Cancer Institute at Florida Hospital, 12722 Research Parkway, Orlando, FL 32826, U.S.A.

\*\*Present address: Department of Biological Chemistry and Molecular Pharmacology, Harvard Medical School, Boston, MA 02115, U.S.A.

been hampered by two different limitations in the methodology:  $^{31}\text{P}$  studies are inhibited by difficulties in resolving resonances within the narrow range of phosphorus chemical shifts, while  $^{113}\text{Cd}$  experiments are limited by poor signal-to-noise ratios. To circumvent these problems, a number of proton-detected experiments are potentially adaptable for measuring these heteronuclear relaxation rates. The proton-detected heteroCOSY experiment is quite sensitive, but the antiphase multiplet structure re-

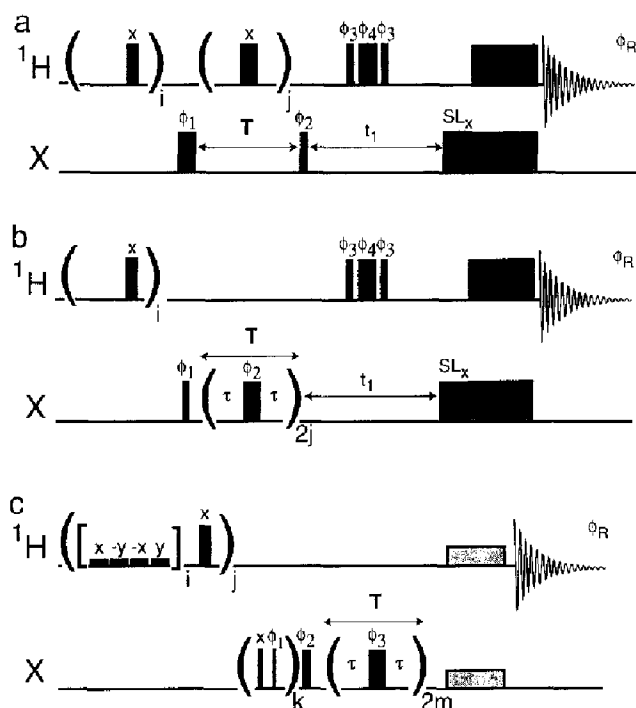


Fig. 1. HeteroTOCSY-based experiments for determining heteronuclear relaxation rates. Unless otherwise noted, large black boxes represent  $180^\circ$  pulses, while thinner black boxes represent  $90^\circ$  pulses.  $\text{SL}_x$  represents a spin-lock pulse. Large dark shaded boxes represent DIPSI-2 (Shaka et al., 1988) heteronuclear mixing sequences applied at high power; lighter grey boxes represent DIPSI-2 sequences applied at lower rf field strength to facilitate selective heteronuclear transfer by heteroTOCSY (Gardner and Coleman, 1994). (a) Two-dimensional inversion recovery heteroTOCSY sequence.  $\phi_1 = \{x, x, x, x, -x, -x, -x, -x\}$ ,  $\phi_2 = \phi_R = \{y, -y\}$ ,  $\phi_3 = \{x, x, -x, -x\}$ ,  $\phi_4 = \{y, y, -y, -y\}$ . *i* Cycle: proton presaturation during relaxation delay; typically 40 cycles were applied with 50 ms between  $180^\circ$  pulses. *j* Cycle: proton saturation during inversion recovery delay  $T$ . (b) Two-dimensional CPMG heteroTOCSY method. *i* Cycle: same as in (a). *j* Cycle: CPMG sequence, repeated as described in Materials and Methods.  $\phi_1 = \phi_R = \{y, -y\}$ ,  $\phi_2 = \{x, x, x, x, -x, -x, -x, -x\}$ ,  $\phi_3$  and  $\phi_4$  cycled as in (a). (c) Selective one-dimensional CPMG heteroTOCSY. *i* Cycle: ORDANTE sequence (Kay et al., 1989) to presaturate  $\text{H}_2\text{O}$  while the proton carrier is upfield of the water resonance. Pulse lengths are  $1/(4D)$ , where  $D$  is the separation (in Hz) between the carrier and the water resonance. *i* Was set to generate 40–50 ms of ORDANTE pulsing while ensuring that *i* is a multiple of 4. *j* Cycle: performs the same function as the *i* cycle in (a) and (b), and is set to a similar duration. *k* Cycle: DANTE-Z (Boudot et al., 1989) using  $22.5^\circ$  pulses ( $k=4$ ) by an appropriate value to ensure that only desirable heteronuclear resonances are excited. *m* Cycle: CPMG sequence, using values as described in Materials and Methods.  $\phi_1 = \{x, -x\}$ ,  $\phi_2 = \{y, y, -y, -y\}$ ,  $\phi_3 = \{x, x, x, x, -x, -x, -x, -x\}$ ,  $\phi_R = \{y, -y, -y, y\}$ .

duces resolution and can attenuate cross-peak intensity (Sklenář et al., 1986). Other experiments, such as HMQC and HSQC, are not as advantageous for either  $^{31}\text{P}$ - $^1\text{H}$  or  $^{113}\text{Cd}$ - $^1\text{H}$  correlations as they are for  $^{13}\text{C}$ - $^1\text{H}$  and  $^{15}\text{N}$ - $^1\text{H}$  correlations in proteins (Byrd et al., 1986). The three-bond scalar coupling constants for  $^{31}\text{P}$ - $^1\text{H}$  and  $^{113}\text{Cd}$ - $^1\text{H}$  cover a wider range ( $^{31}\text{P}$ :  $\sim 0$ – $10$  Hz;  $^{113}\text{Cd}$ :  $\sim 0$ – $60$  Hz) and are significantly smaller than  $^1J$  values for  $^{13}\text{C}$ - $^1\text{H}$  ( $\sim 140$  Hz) and  $^{15}\text{N}$ - $^1\text{H}$  ( $\sim 90$  Hz). Thus, these experiments are harder to optimize, and the long delays necessary for complete refocusing of heteronuclear couplings negate most of the modest sensitivity gain from proton excitation.

An alternative to these methods is offered by the heteronuclear  $J$  cross-polarization spectroscopy (heteroTOCSY) experiment (Bearden and Brown, 1989; Artemov, 1991; Morris and Gibbs, 1991), which has been used to obtain  $^{31}\text{P}$ - $^1\text{H}$  correlations in both oligoribonucleotides (Kellogg, 1992) and oligodeoxyribonucleotides (Kellogg and Schweitzer, 1993), as well as  $^{113}\text{Cd}$ - $^1\text{H}$  correlations in metalloproteins (Gardner and Coleman, 1994). This experiment offers a variety of benefits over the previously described methods, including the fact that it does not require long periods for refocussing, is less sensitive to rf inhomogeneities (Majumdar and Zuiderweg, 1995), and gives rise to absorptive, in-phase cross peaks. Theoretically, this method should offer signal-to-noise improvements of roughly  $(\gamma_{\text{H}}/\gamma_{\text{X}})^{3/2}$  over heteronuclear-detected experiments (Ernst et al., 1987); signal-to-noise enhancements over other proton-detected experiments have also been previously observed (Zuiderweg, 1990; Gardner and Coleman, 1994). The method also allows the observation of several different protons that are  $J$ -coupled to a given heteronucleus, offering improved decay rate statistics and help in resolving peak overlap. In the present study, we have adapted the heteroTOCSY experiment for measuring  $T_1$  and  $T_2$  values both in a selective and a nonselective fashion. These new experiments have been applied here to examine the backbone dynamics of a DNA oligomer modified with an antineoplastic drug, and to characterize the  $^{113}\text{Cd}$  relaxation characteristics in the  $\text{Cys}_5\text{Cd}_2$  LAC9 protein.

## Materials and Methods

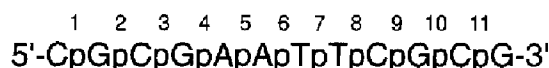
### Sample preparation

The control DNA dodecamer duplex  $d(\text{CGCGAA-TTCGCG})_2$  and the araC-containing dodecamer duplex  $d(\text{CGCGAATT}(\text{araC})d(\text{GCG})_2$  were synthesized and purified as previously described (Schweitzer et al., 1994). The purified ( $>98\%$ ) DNA was dialyzed twice against Chelex-100 (Bio-Rad), lyophilized to dryness, and dissolved in 0.4 ml of buffer containing 50 mM NaCl, 0.5 mM EDTA and 50 mM sodium phosphate, pH 7.0. This solution was repeatedly lyophilized to dryness, first from aqueous buffer and then from 99.96%  $\text{D}_2\text{O}$ . Finally, 0.4

**Control Dodecamer:**

Phosphorus position:

Sequence:

**AraC Dodecamer:**

Phosphorus position:

Sequence:

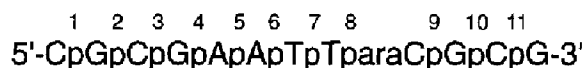


Fig. 2. Sequence and numbering scheme for the control and araC dodecamers. Only one strand of the selfcomplementary duplex is shown.

ml of 99.996% D<sub>2</sub>O was added to give a final duplex concentration of ca. 5 mM.

LAC9(61) is a 61-residue internal fragment of the LAC9 protein (Lys<sup>85</sup> to Arg<sup>144</sup>, with an N-terminal methionine residue added during cloning). LAC9(61) was overexpressed in *Escherichia coli* and purified as previously described (Pan et al., 1990; Gardner and Coleman, 1994). The <sup>113</sup>Cd<sub>2</sub> form of LAC9 was generated by incubating protein samples with a three- to fivefold molar excess of <sup>113</sup>CdCl<sub>2</sub> (95% isotopically enriched in <sup>113</sup>Cd) for 24 h, followed by dialysis against metal-free buffer. The sample used for NMR measurements had a protein concentration of 3 mM in 10 mM sodium phosphate buffer and 500 mM NaCl, pH 5.7.

*NMR spectroscopy*

All NMR experiments were carried out on a Bruker AM-500 spectrometer (500.13, 202.45 and 110.92 MHz for protons, phosphorus and cadmium, respectively). <sup>31</sup>P resonances were referenced to an external sample of trimethylphosphate, <sup>113</sup>Cd resonances were referenced to an external sample of 1.0 M Cd(ClO<sub>4</sub>)<sub>2</sub>, and <sup>1</sup>H resonances were referenced to an external sample of sodium-2,2-dimethyl-2-silapentane-5-sulfonate (DSS) in a buffer identical to that of the NMR sample.

The <sup>31</sup>P inverse recovery (IR)-heteroTOCSY and <sup>31</sup>P Carr-Purcell-Meiboom-Gill (CPMG)-heteroTOCSY experiments were carried out using the pulse schemes shown in Figs. 1a and b, respectively. In these experiments, four power settings on two channels were used; the decoupler channel was used for the proton pulses at high power for the presaturation sequence and at a lower power for the remaining pulses. The presaturation sequence is designed to eliminate all proton magnetization prior to the first heteronuclear pulse (Kellogg, 1992).\* The transmitter (set to <sup>31</sup>P) was equipped with a fast low-power switch and a fast-switch linear amplifier. The power level of the transmitter was adjusted manually to meet the Hartmann-

Hahn matching condition during the contact time of each experiment (Kellogg, 1992). Data were recorded in the phase-sensitive mode with time-proportional phase incrementation (TPPI; Marion and Wüthrich, 1983).

In the <sup>31</sup>P IR-heteroTOCSY experiment, recovery of magnetization was measured at T = 0.05, 0.5, 1.0, 1.5, 2.0, 3.0, 4.0, 5.0, and 6.0 s. In the <sup>31</sup>P CPMG-heteroTOCSY experiments, a CPMG sequence was used during the relaxation delay period using τ = 2.5 ms, and setting T = 10, 20, 30, 40, 60, 80, 100, 120, 200, and 250 ms. Data were acquired at each T value with 1024 points in t<sub>2</sub> and with 16 transients for each of the 48 t<sub>1</sub> points. Each experiment was carried out using <sup>31</sup>P and <sup>1</sup>H sweep widths of 252.5 and 4386 Hz, respectively. Heteronuclear transfer between phosphorus and protons was achieved using a simultaneous DIPSI-2 mixing sequence (Shaka et al., 1988), applied for 49.0 ms with a 4.2 kHz radiofrequency field strength.

Parameters for the selective <sup>113</sup>Cd CPMG-heteroTOCSY experiment (Fig. 1c) were chosen using the guidelines for the analogous selective heteroTOCSY experiment (Gardner and Coleman, 1994). Selective excitation of the <sup>113</sup>Cd nucleus was accomplished using a DANTE-Z pulse scheme (Boudot et al., 1989) consisting of π/4 pulses separated by 151 μs; this cycle was repeated four times. T<sub>2</sub> measurements used a CPMG sequence during the relaxation delay period with τ = 1.5 ms, and setting T = 6.5, 13.0, 19.4, 25.9, 32.4, 38.9, 51.8, and 64.8 ms. T<sub>1ρ</sub> measurements used a 1.3 kHz rf field strength spin-lock pulse during relaxation delays of T = 6, 12, 18, 24, 30, 36, 48, and 60 ms. Selective heteronuclear transfer between cadmium and protons was achieved using a DIPSI-2 mixing sequence, applied simultaneously to both channels with an rf field strength of 2.1 kHz and a duration of 14.0 ms. A total of 512 scans were recorded for each time point. A 1D <sup>113</sup>Cd spectrum (see the inset of Fig. 6) of LAC9(61) was collected using 3300 scans with a recycle time of 0.4 s and a 60° cadmium pulse width.

NMR data were processed using the program FELIX, v. 2.1 (Biosym Technologies, San Diego, CA). For the <sup>31</sup>P heteroTOCSY experiments, the t<sub>1</sub> dimension was zero-filled to 128 points; no zero-filling was used in the t<sub>2</sub> dimension. The residual water signal was removed using deconvolution (Marion et al., 1989). Data sets were apo-

\*We have repeated several of our experiments using 120° presaturation pulses (Markley et al., 1971) and have obtained higher quality proton saturation. However, no differences were observed between relaxation parameter values obtained with 180° or 120° presaturation pulses.

dized with a squared sine-bell window shifted 90° in both dimensions prior to Fourier transformation. The first time point of each dimension was estimated by linear prediction. Cross peaks were manually picked and volumes were measured using FELIX. For the  $^{13}\text{C}$  heteroTOSY experiments, time-domain FIDs were subjected to linear prediction of the first two datapoints and 5 Hz exponential linebroadening prior to Fourier transformation. Baselines of the spectra were fit to fifth-order polynomial equations in order to improve flatness, after which peak volumes were measured. All  $T_1$  decays were fit to a three-parameter exponential equation of the form:  $I(T) = I_\infty - [I_\infty - I_0] \exp(-T/T_1)$ , while  $T_2$  and  $T_{1\rho}$  decays were fit to the two-parameter equation  $I(T) = I_0 \exp(-T/T_2)$  and  $I(T) = I_0 \exp(-T/T_{1\rho})$ , respectively, where  $I_\infty$  is the peak volume at infinite relaxation delay and  $I_0$  is the peak volume at a relaxation delay of 0 s.

## Results

### $^{31}\text{P}$ relaxation measurements: AraC

The nucleoside analog 1- $\beta$ -D-arabinofuranosylcytosine (araC) is a potent agent in the treatment of various forms of human leukemia (Bodey et al., 1969; Frei et al., 1969). AraC is converted by cellular kinases into the active metabolite araCTP (Coleman et al., 1975; Hande and Chabner, 1978), which in turn is incorporated into cellular genomic DNA (Kufe et al., 1980; Major et al., 1982). It is this misincorporation of araC into DNA that is the lethal event in cells (Kufe et al., 1980). In vitro experiments have shown that araC at a 3' primer terminus or in the template strand of a DNA substrate strongly inhibits replication by the Klenow fragment of *E. coli* DNA polymerase I, T4 polymerase, DNA polymerase  $\alpha$ , and reverse transcriptase (Mikita and Beardsley, 1988; Perrino and Mekosh, 1992). A high-resolution X-ray structure of a B-type decamer duplex containing araC has been described by Gao et al. (1991). In addition, our laboratory has recently determined the NMR solution structure of a dodecamer duplex containing araC (Schweitzer et al., 1994). Both studies indicated that incorporation of araC into a B-DNA context produces a rather small amount of distortion and concluded that it would be difficult to correlate this distortion with the biochemical effects of araC. In the present study, we analyze the effect of araC on the structure and dynamics of the sugar-phosphate backbone of DNA by measuring the longitudinal and transverse  $^{31}\text{P}$  relaxation rates in an araC-containing duplex and a control duplex.

The control and araC-containing DNA duplexes used in this study have been used previously in structural work (Fig. 2; Schweitzer et al., 1994). One-dimensional  $^{31}\text{P}$  spectra of these oligomers acquired at either 4.7 T or 11.74 T indicated that the dispersion of the resonances is insufficient to accurately determine  $^{31}\text{P}$  relaxation rates

using conventional one-dimensional methods (not shown). Most of the phosphorus resonances were found to be clustered in a 0.5 ppm range. Only one phosphorus resonance in the araC duplex was clearly resolved from the other 10 resonances; using a heteroTOSY-based assignment strategy, this resonance has previously been assigned to the phosphorus located between residues dC(11) and dG(12) (Schweitzer et al., 1994). One-dimensional  $^{31}\text{P}$  inversion-recovery and CPMG experiments at 202.45 MHz gave  $T_1$  and  $T_2$  values of 1.35 s and 71 ms, respectively, for the dC(11) phosphorus (Fig. 3).

In our previous work, most of the phosphorus resonances in the two oligomers could be resolved in the 2D

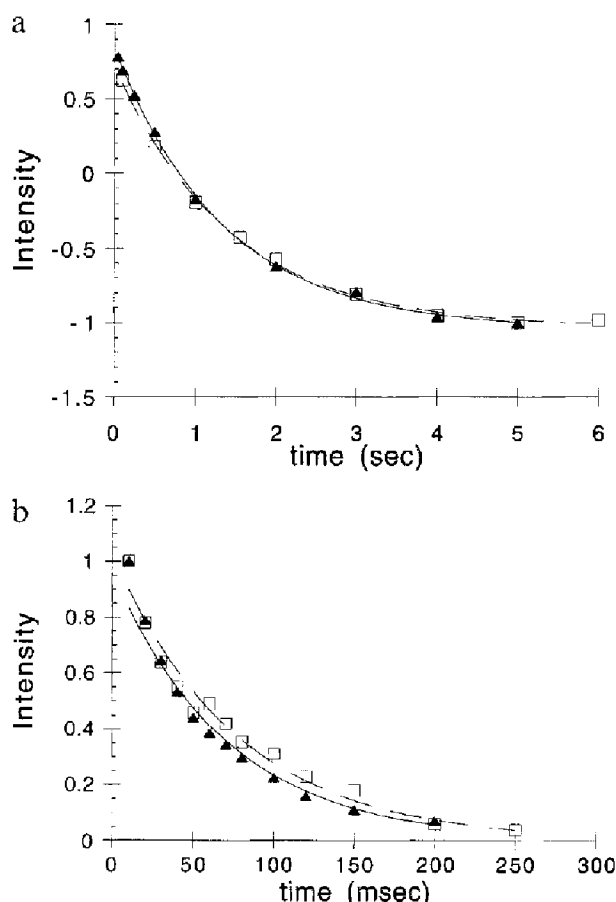


Fig. 3. (a) 1D versus 2D determination of  $^{31}\text{P}$   $T_1$  values. The data shown are for the dC(11) phosphorus resonance in the araC duplex. One-dimensional data (filled triangles) were acquired with an inversion-recovery  $^{31}\text{P}$ -detected pulse sequence. Two-dimensional data (open squares) were obtained with the pulse sequence described in Materials and Methods. The 1D and 2D data sets were acquired sequentially, without removing the sample from the magnet.  $T_1$  values obtained from the 1D and 2D data sets were 1.35 and 1.40 s, respectively. (b) 1D versus 2D determination of  $^{31}\text{P}$   $T_2$  values. The data shown are for the dC(11) phosphorus resonance in the araC duplex. One-dimensional data (filled triangles) were acquired with an inversion-recovery  $^{31}\text{P}$ -detected pulse sequence. Two-dimensional data (open squares) were obtained with the pulse sequence described in Materials and Methods. The 1D and 2D data sets were acquired sequentially, without removing the sample from the magnet.  $T_2$  values obtained from the 1D and 2D data sets were 71 and 76 ms, respectively.

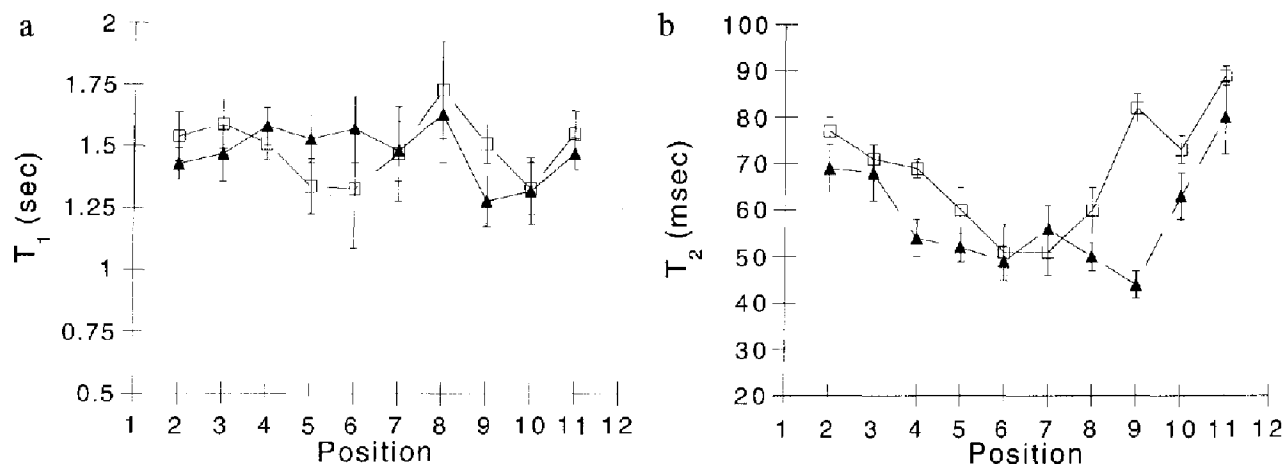


Fig. 4. (a)  $^{31}\text{P}$   $T_1$  values and (b)  $^{31}\text{P}$   $T_2$  values for the control and araC dodecamers. Data for the control duplex (open squares) and for the araC duplex (filled triangles) are plotted as a function of phosphorus position. Each point is the mean of two (a) or three (b) separate experiments.

$^1\text{H}$ - $^{31}\text{P}$  heteroTOCSY experiment (Kellogg and Schweitzer, 1993; Schweitzer et al., 1994). For the present study, we modified the heteroTOCSY pulse sequence so that the initial pulse on phosphorus was replaced with an inversion-recovery sequence or a CPMG sequence to allow the measurement of the  $^{31}\text{P}$   $T_1$  and  $T_2$  values, respectively. The mixing times in these experiments were kept short, in order to eliminate interresidue sequential cross peaks (Kellogg and Schweitzer, 1993) and thus improve resolution. We were pleased to observe that the  $^{31}\text{P}$   $T_1$  and  $T_2$  values for the dC(11) phosphorus of the araC duplex, measured by either the conventional 1D or the new 2D method, were nearly identical (see Fig. 3).

$^{31}\text{P}$   $T_1$  and  $T_2$  values measured by the heteroTOCSY-based experiment for the remainder of the phosphorus resonances (except for dC(1), which was obscured by the residual solvent signal) are shown in Figs. 4a and b for the control and araC duplexes, respectively. In Fig. 4a, it can be seen that the  $^{31}\text{P}$   $T_1$  values show little variation with phosphorus position. Also, few significant differences appear to be present between the control and araC-modified DNA fragments, except at position 9, where the  $T_1$  value at the araC incorporation site is slightly less than that of the control. The  $T_2$  values, on the other hand, do appear to vary considerably with position (Fig. 4b). A clear pattern can be observed:  $T_2$  values are low (ca. 50 ms) in the center of the helix and gradually increase on going to the ends of the helix. This pattern is observable in both the control and the araC duplex. Two sites, one at the araC incorporation site and one at position 4, display highly significant differences in  $T_2$  values in the control and araC duplexes. It should be noted that in the selfcomplementary duplex, position 4 is opposite the araC site on the complementary strand.

In Fig. 5, the  $T_2$  values for the control and araC duplexes are plotted versus  $^{31}\text{P}$  chemical shift. It can be seen in this plot that the  $T_2$  values appear to be highly corre-

lated ( $R=0.91$ ) with  $^{31}\text{P}$  chemical shift. Interestingly, this correlation is preserved in the control and araC duplexes, despite some fairly large differences between some of the  $^{31}\text{P}$  chemical shifts (e.g., phosphates 9 and 10 (Schweitzer et al., 1994)). The possible significance of this observation will be discussed in more detail below.

#### $^{113}\text{Cd}$ relaxation measurements: LAC9

Over 25 yeast transcription factors contain a conserved motif of six cysteines in their DNA-binding domains. This was originally identified in the *Saccharomyces cerevisiae* protein GAL4, a transcriptional activator of enzymes involved in galactose metabolism (Johnston, 1987). Domains containing this motif must bind Zn(II) or Cd(II) for the protein to have specific DNA-binding activity (Pan and Coleman, 1989). Previous  $^{113}\text{Cd}$  NMR studies demonstrated the involvement of all six conserved cysteines in binding two metal atoms in a binuclear cluster arrangement (Pan and Coleman, 1990; Gadhavi et al., 1991; Gardner et al., 1991). Subsequent structural studies of the GAL4 DNA-binding domain showed that the protein structure of this domain organizes around this cluster (Baleja et al., 1992; Kraulis et al., 1992; Shirakawa et al., 1993) and that these domains interact with their DNA-binding sites by utilizing groups oriented by the first three conserved cysteine ligands (Marmorstein et al., 1992).

To better characterize the structural and dynamic features of the metal-binding sites in this motif, we investigated the relaxation properties of the two  $^{113}\text{Cd}$  nuclei bound by one of these proteins. We focused our studies on the DNA-binding domain from the *Kluyveromyces lactis* LAC9 protein, a  $\text{Cys}_6\text{Zn}_2$  motif-containing transcription factor that is highly homologous to GAL4, both in amino acid sequence and in biological function (Pan et al., 1990). We previously used  $^{113}\text{Cd}$ - $^1\text{H}$  heteroTOCSY methods to assign the metal-liganding cysteines in  $^{113}\text{Cd}_2$ -

LAC9(61) (Gardner and Coleman, 1994), demonstrating the feasibility of using selective heteronuclear correlation methods to study the cadmium-liganding environment. Metalloprotein systems like this one typically have a small number of heteronuclei present; as such, we have developed 1D selective NMR techniques for studying the metal-protein interactions, as the additional resolution offered by a second heteronuclear dimension is not needed. To monitor  $^{113}\text{Cd}$  relaxation rates, we modified our selective heteroTOCSY protocols in a manner analogous to the 2D methods modified to probe phosphorus relaxation rates by inserting the appropriate sequences to generate and follow the decay of the desired type of heteronuclear magnetization (CPMG for  $T_2$  determinations; spin-lock for  $T_{1\rho}$ ; Fig. 1c). After allowing relaxation to proceed for a given amount of time, we transfer cadmium magnetization to the cysteine  $\beta$  protons ( $^1J_{\text{Cd-H}}$ : 5–60 Hz) for detection.

We used a 1D CPMG selective heteroTOCSY experiment to determine the cadmium relaxation rates of  $\text{Cd}_2\text{-LAC9(61)}$ .  $T_2$  relaxation times were measured for each of the cadmium nuclei separately (Fig. 6). By fitting these intensity curves to an exponential decay equation, we determined  $T_2$  values of  $21.7 \pm 1.2$  ms for the downfield cadmium resonance (706 ppm) and  $14.7 \pm 0.4$  ms for the upfield resonance (691 ppm). These values were lower than those observed in measurements of the  $^{113}\text{Cd}$   $T_{1\rho}$  values ( $24.5 \pm 1.0$  ms (706 ppm),  $15.9 \pm 0.3$  ms (691 ppm)). Due to the increase in sensitivity offered by the proton detection used in these methods, we were able to conduct this series of experiments in a shorter amount of time (less than 3 h per heteronucleus) than a comparable cadmium-detected experiment would have taken.

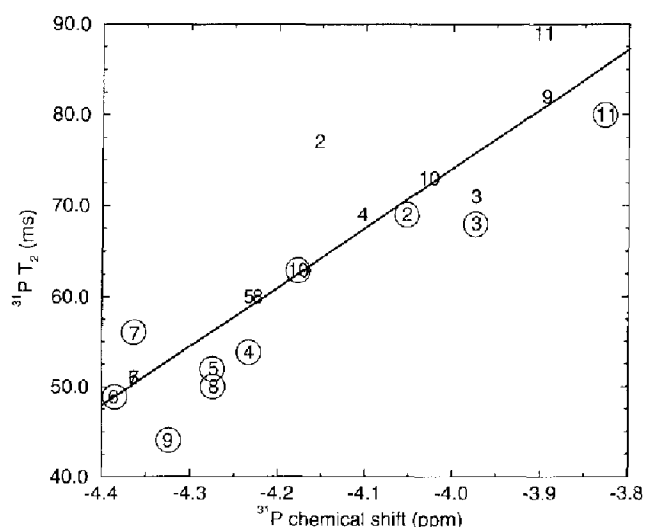


Fig. 5.  $^{31}\text{P}$   $T_2$  values versus  $^{31}\text{P}$  chemical shift. Numbers represent the position of the phosphate in the DNA sequence.  $^{31}\text{P}$  chemical shifts for the control (position numbers not circled) and araC (position numbers circled) duplexes were taken from Schweitzer et al. (1994). The drawn line is the best fit line (correlation coefficient  $R=0.91$ ) determined by linear regression.

## Discussion

In this study, we have demonstrated that heteroTOCSY-based experiments can be employed to measure heteronuclear relaxation rates in DNA oligonucleotides and proteins. These experiments give results that are very similar to those obtained by conventional 1D techniques for phosphorus and cadmium resonances that can be resolved in 1D spectra. For phosphorus relaxation measurements, the advantage of the 2D heteroTOCSY-based experiment over the 1D experiments is the ability to resolve most, if not all, of the individual phosphorus resonances in small to moderately sized oligodeoxyribonucleotides. To the best of our knowledge, the relaxation data presented in Figs. 4a and b represent the most complete set of relaxation values for oligonucleotides of this size. In addition, this determination of  $^{113}\text{Cd}$  transverse relaxation times represents one of the first direct measurements of cadmium  $T_2$  values in a metalloprotein system. Most values reported previously have been derived from linewidth determinations in  $^{113}\text{Cd}$  1D spectra, which suffer from poor signal-to-noise ratios. Below, we discuss how the information obtained using these new techniques provides insights into the dynamic processes of the systems under study.

### $^{31}\text{P}$ results

The availability of a virtually complete set of relaxation data for an oligonucleotide allows a more thorough analysis of the DNA backbone than has been previously possible. We were unable to detect a steady-state  $^{31}\text{P}\{^1\text{H}\}$  NOE (data not shown), which is in agreement with earlier work by Williamson and Boxer (1989) who showed that at 11.74 T, both theory and experiment indicated that <3% of the total phosphorus relaxation was due to dipolar interaction with protons. The  $T_1$  and  $T_2$  relaxation rates due to the CSA mechanism for an isotropically tumbling molecule that has an axially symmetric CSA tensor are given by:

$$1/T_{1\text{CSA}} = 1/15 \{ \omega P^2 \Delta \sigma^2 J(\omega_p) \} \quad (1)$$

and

$$1/T_{2\text{CSA}} = 1/90 \{ \omega P^2 \Delta \sigma^2 [3J(\omega_p) + 4J(0)] \} \quad (2)$$

(Abragam, 1961). These equations can be simplified to the following expression, relating the phosphorus relaxation rates to the effective rotational correlation time:

$$\tau_c = \frac{1}{\omega_p} \left[ \frac{3}{2} \left( \frac{T_1}{T_2} \right) - \frac{7}{4} \right]^{1/2} \quad (3)$$

Equation 3 is true only when  $\omega_p \tau_c > 1$  (Williamson and Boxer, 1989). If the  $T_1$  and  $T_2$  values for the control oli-

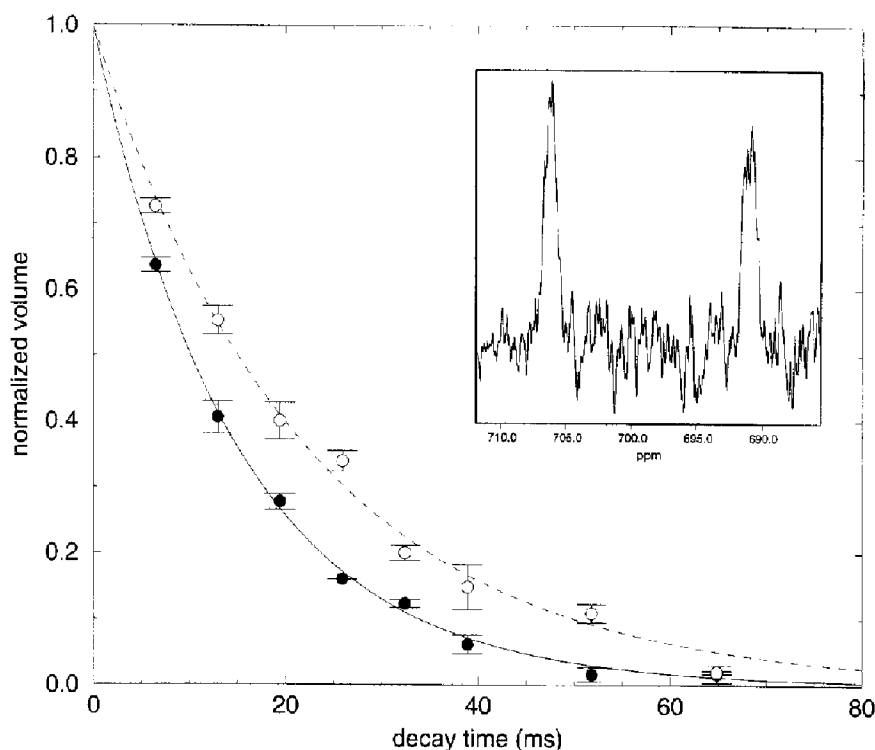


Fig. 6. Determination of  $^{113}\text{Cd}$  transverse relaxation ( $T_2$ ) times in LAC9(61). Data were generated using the selective CPMG heteroTOCSY experiment (Fig. 1c), using parameters given in Materials and Methods. Each data point is the mean of two independently acquired experiments. The  $T_2$  values were determined by fitting the decay of the cysteine  $\beta$ -proton peak volumes as a function of the total delay period  $T$ .  $T_2$  values are  $21.7 \pm 1.2$  ms (dashed line, Cys $^{112}$ , Cys $^{115}$  and Cys $^{122}$   $\beta$ -protons coupled to cadmium at 706 ppm) and  $14.7 \pm 0.4$  ms (solid line, Cys $^{95}$ , Cys $^{98}$  and Cys $^{105}$   $\beta$ -protons coupled to cadmium at 691 ppm). Inset: a directly detected 1D  $^{113}\text{Cd}$  NMR spectrum of LAC9(61), used to directly obtain  $T_2^*$  from the half-height line widths. Data were generated using the parameters described in Materials and Methods.

igonucleotide are averaged and used in Eq. 3, a value of 4.25 ns is obtained for  $\tau_c$ . This value is exactly identical to that previously calculated for this duplex from NOESY data (Schweitzer et al., 1994). The agreement between the rotational correlation times obtained from phosphorus and proton relaxation supports the conclusion that all of the phosphorus relaxation was due to CSA, and that there is little contribution to the  $^{31}\text{P}$   $T_2$  values from chemical exchange.

In B-type DNA, when the P-O3' ( $\zeta$ ) conformation is  $g^-(-60^\circ)$ , the C-O3' conformation ( $\epsilon$ ) is usually  $t(180^\circ)$  (Dickerson and Drew, 1981). This  $\epsilon(t)$ ,  $\zeta(g^-)$  state (also known as the  $B_I(t,g)$  conformation (Dickerson and Drew, 1981)) is the most common backbone conformation, and represents the low-energy phosphate state (Gorenstein, 1987). The other common conformation is the  $\epsilon(g^-)$ ,  $\zeta(t)$  or  $B_{II}$  conformation, which has been shown by molecular orbital calculations to have a 1.0 kcal/mol higher energy than the  $B_I$  conformation (Gorenstein et al., 1977; Gorenstein, 1987). A 'crankshaft' motion interconverts  $B_I$  and  $B_{II}$  with only a modest movement of the phosphate; molecular dynamics simulations have shown that this conversion can occur on a picosecond time scale (Kaluarachchi et al., 1991).

Roongta et al. (1990) found a linear relationship between  $^{31}\text{P}$  chemical shift and the C4'-C3'-O3'-P torsional

angle  $\epsilon$  in a series of short oligodeoxyribonucleotides. From these results, it was estimated that a phosphate in a purely  $B_I$  conformational state should have a  $^{31}\text{P}$  chemical shift of ca.  $-4.6$  ppm, whereas a phosphate in a purely  $B_{II}$  conformational state should have a  $^{31}\text{P}$  chemical shift of ca.  $-3.0$  ppm (Roongta et al., 1990). An analysis of  $^{31}\text{P}$  chemical shifts and  $J_{\text{H}3\text{-P}}$  coupling constants also revealed a positional effect on backbone conformation – phosphates at the end of the helix tend to have more downfield  $^{31}\text{P}$  chemical shifts and more  $B_{II}$  character, while phosphates in the interior will have upfield chemical shifts and nearly 100%  $B_I$  conformation (Roongta et al., 1990). We have observed the same positional effects on the  $^{31}\text{P}$  chemical shifts in the two duplexes used in this study (Schweitzer et al., 1994); a notable deviation occurs at the site of araC incorporation, where the phosphorus resonance is shifted 0.4 ppm upfield.

It has been suggested that the change from a 'pure'  $B_I$  conformation in the interior of the helix to a mixture of  $B_I$  and  $B_{II}$  conformations at the ends of the helix is due to increased conformational freedom at the ends (Gorenstein, 1987; Roongta et al., 1990). The data presented in this paper support this hypothesis. Figure 4 shows that the  $^{31}\text{P}$   $T_2$  values are lower in the interior of the helix, consistent with the greater conformational constraint imposed by the stacked, base-paired geometry. In Fig. 5,

$^{31}\text{P}$   $T_2$  values are shown to be highly correlated with  $^{31}\text{P}$  chemical shift; extrapolation from the work by Gorenstein and co-workers suggests that the lower  $T_2$  values are associated with a 'static' or stable  $B_1$  conformation. On the other hand, a higher  $T_2$  value implies more frequent transitions to a  $B_{11}$  conformation. Thus, the lower  $T_2$  value and the upfield  $^{31}\text{P}$  chemical shift of the phosphate at position 9 in the araC duplex indicate a more stable  $B_1$  conformation than found for the corresponding phosphate in the control duplex. To a lesser extent, this is also the case for the phosphate at position 4. Alternatively, the large difference in  $T_2$  values at these positions may be indicative of an intermediate exchange process, although little, if any, broadening of these phosphorus resonances could be observed.

Preliminary analysis of the relaxation rates using the model-free formalism (Lipari and Szabo, 1982) with fast internal motions suggests that the observed changes in  $T_1$  and  $T_2$  along the length of the DNA duplex can be attributed chiefly to a decrease in the  $S^2$  order parameter at the ends of the helix.  $S^2$  is substantially increased at both positions 4 and 9 of the araC duplex, supporting the conclusion that backbone mobility is decreased at the site of araC incorporation. Further studies at different field strengths and on DNA duplexes of different sizes are in progress to investigate this phenomenon in more detail.

#### $^{113}\text{Cd}$ results

One interesting feature of the GAL4 DNA-binding domain structure (Baleja et al., 1992; Kraulis et al., 1992; Marmorstein et al., 1992) is the presence of a pseudodyad symmetry axis running through the center of the zinc binuclear cluster. This symmetry is strongest in the immediate vicinity of the metal-sulfur complex, with two tetrahedral arrangements of ligands around the metal atoms. It is further reflected in a symmetric network of hydrogen bonds between backbone amide protons and the cysteine sulfur atoms (Kraulis et al., 1992; Mau et al., 1992; K.H. Gardner and J.E. Coleman, unpublished results) and in the arrangement of protein secondary structural elements.

Although the presence of this symmetry suggests that the two metal-binding sites are equivalent, several functional differences have been observed between them. Maximal DNA-binding affinity by GAL4 is observed when two equivalents of zinc are bound, yielding  $K_d$  values of approximately 10 nM for GAL4(149\*) binding to a  $\text{UAS}_G$  site (Rodgers and Coleman, 1994). However, one of the zinc atoms can be removed from  $\text{Zn}_2\text{GAL4}$  fragments by extensively dialyzing the protein against an EDTA-containing buffer (Gardner et al., 1991; Rodgers and Coleman, 1994), resulting in a protein that binds DNA with a four- to eightfold reduced affinity compared to the  $\text{Zn}_2$  species. Additionally, experiments examining the metal exchange kinetics using radioactive isotopes of either zinc or cadmium exhibit two different rate constants,

demonstrating that the two metal-binding sites have differential lability (Rodgers and Coleman, 1994). Taken together, these results suggest a greater degree of dissimilarity than the structural studies have previously identified.

These differences appear to be echoed in the different relaxation rates observed between the two  $^{113}\text{Cd}$  nuclei bound to the LAC9 cysteine cluster. Possible reasons for the differences include both geometric and dynamical sources; we are currently evaluating other relaxation data to identify the contributions of these two possibilities. An interesting observation is that the  $T_2$  values determined via the heteroTOCSY technique are substantially longer than the  $T_2^*$  values calculated from the half-height widths of 1D  $^{113}\text{Cd}$  spectra (see inset in Fig. 6). Interpreting the line widths of these spectra as  $T_2^* = 1/(\Delta\nu_{1/2}\pi)$  generates values of approximately 3 ms for both nuclei. As noted previously (Kördel et al., 1992), many other cadmium-substituted metalloprotein systems display short  $T_2^*$  times, on the order of 1–10 ms, that have been attributed to exchange between different protein conformations. This mechanism is also supported by the observation that  $T_{1\rho} > T_2$ , potentially due to the refocusing of exchange processes on the millisecond time scale. We will be conducting further research to define this phenomenon and its sources.

#### Acknowledgements

We would like to acknowledge the following contributors: J.E. Coleman and G. Peter Beardsley for ongoing support and valuable discussions, L.E. Kay, D.G. Gorenstein, and members of the Coleman laboratory for critical reading of the manuscript, J.M. Armitage for discussions on cadmium-113 relaxation mechanisms, and T. Mikita for preparation of the araC phosphoramidite. B.I.S. was supported by National Institutes of Health Grant F32 AI08472 and is a Leukemia Society of America Special Fellow. G.T.-K. was supported by NIH Grant GM-41651 to Peter B. Moore (Department of Chemistry, Yale University). K.H.G. was supported by a predoctoral fellowship from the Howard Hughes Medical Institute and by NIH Grant DK-09070 to Joseph E. Coleman (Department of Molecular Biophysics and Biochemistry, Yale University).

#### References

- Abragam, A. (1961) *The Principles of Nuclear Magnetism*, Clarendon Press, Oxford.
- Artemov, D.Y. (1991) *J. Magn. Reson.*, **91**, 405–407.
- Baleja, J.D., Marmorstein, R., Harrison, S.C. and Wagner, G. (1992) *Nature*, **356**, 450–453.
- Bearden, D.W. and Brown, L.R. (1989) *Chem. Phys. Lett.*, **163**, 432–436.
- Bodey, G., Freireich, E., Monto, R. and Hewlett, J. (1969) *Cancer Chemother. Rep.*, **53**, 59–66.



- Boudot, D., Canet, D., Brondeau, J. and Boubel, J.C. (1989) *J. Magn. Reson.*, **83**, 428–439.
- Byrd, R.A., Summers, M.F., Zon, G., Fouts, C.S. and Marzilli, L.G. (1986) *J. Am. Chem. Soc.*, **108**, 504–505.
- Coleman, C.N., Stoller, R.G., Drake, J.C. and Chabner, B.A. (1975) *Blood*, **46**, 791–803.
- Dickerson, R.E. and Drew, H.R. (1981) *J. Mol. Biol.*, **149**, 761–786.
- Ernst, R.R., Bodenhausen, G. and Wokaun, A. (1987) *Principles of Nuclear Magnetic Resonance in One and Two Dimensions*, Clarendon Press, Oxford, p. 468.
- Frei, E., Bickers, J., Lane, M., Leary, W. and Talley, R. (1969) *Cancer Res.*, **29**, 1325–1332.
- Gadhavi, P.L., Davis, A.L., Povey, J.F., Keeler, J. and Laue, E.D. (1991) *FEBS Lett.*, **281**, 223–226.
- Gao, Y.-G., Van der Marel, G.A., Van Boom, J.H. and Wang, A.H.-J. (1991) *Biochemistry*, **30**, 9922–9931.
- Gardner, K.H., Pan, T., Narula, S., Rivera, E. and Coleman, J.E. (1991) *Biochemistry*, **30**, 11292–11302.
- Gardner, K.H. and Coleman, J.E. (1994) *J. Biomol. NMR*, **4**, 761–774.
- Gorenstein, D.G., Luxon, B.A. and Findlay, J.B. (1977) *Biochim. Biophys. Acta*, **475**, 184–190.
- Gorenstein, D.G. (1987) *Chem. Rev.*, **87**, 1047–1077.
- Hande, K.R. and Chabner, B.A. (1978) *Cancer Res.*, **38**, 579–585.
- Johnston, M. (1987) *Nature*, **328**, 353–355.
- Kaluarachchi, K., Meadows, R.P. and Gorenstein, D.G. (1991) *Biochemistry*, **30**, 8785–8797.
- Kay, L.E., Marion, D. and Bax, A. (1989) *J. Magn. Reson.*, **84**, 72–84.
- Kellogg, G.W. (1992) *J. Magn. Reson.*, **98**, 176–182.
- Kellogg, G.W. and Schweitzer, B.I. (1993) *J. Biomol. NMR*, **3**, 577–595.
- Kördel, J., Johansson, C. and Drakenberg, T. (1992) *J. Magn. Reson.*, **100**, 581–587.
- Kraulis, P.J., Raine, A.R.C., Gadhavi, P.L. and Laue, E.D. (1992) *Nature*, **356**, 448–450.
- Kufe, D.W., Major, P.P., Egan, E.M. and Beardsley, G.P. (1980) *J. Biol. Chem.*, **255**, 8997–9000.
- Lipari, G. and Szabo, A. (1982) *J. Am. Chem. Soc.*, **104**, 4546–4559.
- Major, P.P., Egan, E.M., Herrick, D. and Kufe, D.W. (1982) *Biochem. Pharmacol.*, **31**, 2937–2940.
- Majumdar, A. and Zuiderweg, E.R.P. (1995) *J. Magn. Reson. Ser. A*, **113**, 19–31.
- Marion, D. and Wüthrich, K. (1983) *Biochem. Biophys. Res. Commun.*, **113**, 967–974.
- Marion, D., Ikura, M. and Bax, A. (1989) *J. Magn. Reson.*, **84**, 425–430.
- Markley, J.L., Horsley, W.J. and Klein, M.P. (1971) *J. Chem. Phys.*, **55**, 3604–3607.
- Marmorstein, R., Carey, M., Ptashne, M. and Harrison, S.C. (1992) *Nature*, **356**, 408–414.
- Mau, T., Baleja, J.D. and Wagner, G. (1992) *Protein Sci.*, **1**, 1403–1412.
- Mikita, T. and Beardsley, G.P. (1988) *Biochemistry*, **27**, 4698–4705.
- Morris, G.A. and Gibbs, A. (1991) *J. Magn. Reson.*, **91**, 444–449.
- Pan, T. and Coleman, J.E. (1989) *Proc. Natl. Acad. Sci. USA*, **86**, 3145–3149.
- Pan, T. and Coleman, J.E. (1990) *Proc. Natl. Acad. Sci. USA*, **87**, 2077–2081.
- Pan, T., Halvorsen, Y.-D., Dickson, R.C. and Coleman, J.E. (1990) *J. Biol. Chem.*, **265**, 21427–21429.
- Perrino, F.W. and Mekosh, H.L. (1992) *J. Biol. Chem.*, **267**, 23043–23051.
- Rodgers, K.R. and Coleman, J.E. (1994) *Protein Sci.*, **3**, 608–619.
- Roongta, V.A., Jones, C.R. and Gorenstein, D.G. (1990) *Biochemistry*, **29**, 5245–5258.
- Schweitzer, B.I., Mikita, T., Kellogg, G.W., Gardner, K.H. and Beardsley, G.P. (1994) *Biochemistry*, **33**, 11460–11475.
- Shaka, A.J., Lee, C.J. and Pines, A. (1988) *J. Magn. Reson.*, **77**, 274–293.
- Shirakawa, M., Fairbrother, W.J., Serikawa, Y., Ohkubo, T., Kyo-goku, Y. and Wright, P.E. (1993) *Biochemistry*, **32**, 2144–2153.
- Sklenář, V., Miyashiro, H., Zon, G., Miles, H.T. and Bax, A. (1986) *FEBS Lett.*, **208**, 94–98.
- Williamson, J.R. and Boxer, S.G. (1989) *Biochemistry*, **28**, 2819–2831.
- Zuiderweg, E.R.P. (1990) *J. Magn. Reson.*, **89**, 533–542.